ELSEVIER

Mechanisms of Development 113 (2002) 15–28

www.elsevier.com/locate/modo

Rotatin is a novel gene required for axial rotation and left–right specification in mouse embryos

Anja M. Faisst, Gonzalo Alvarez-Bolado, Dieter Treichel, Peter Gruss*

Department of Molecular Cell Biology, Max-Planck Institute of Biophysical Chemistry, Am Fassberg 11, 37077 Goettingen, Germany

Received 25 September 2001; received in revised form 18 December 2001; accepted 19 December 2001

Abstract

The genetic cascade that governs left–right (L–R) specification is starting to be elucidated. In the mouse, the lateral asymmetry of the body axis is revealed first by the asymmetric expression of *nodal*, *lefty2* and *pitx2* in the left lateral plate mesoderm of the neurulating embryo. Here we describe a novel gene, *rotatin*, essential for the correct expression of the key L–R specification genes *nodal*, *lefty* and *Pitx2*. Embryos deficient in rotatin show also randomized heart looping and delayed neural tube closure, and fail to undergo the critical morphogenetic step of axial rotation. The amino acid sequence deduced from the cDNA is predicted to contain at least three transmembrane domains. Our results show a novel key player in the genetic cascade that determines L–R specification, and suggest a causal link between this process and axial rotation.

Keywords: Axial rotation; Mouse; Gene trap; β-Galactosidase reporter; Left–right development; *nodal*; *lefty-2*; *Pitx2*

1. Introduction

The internal visceral organs of vertebrates are arranged at both sides of the body midline with a characteristic asymmetry whose genetic basis is beginning to be unveiled. At the end of gastrulation, the primordia of the respiratory and digestive organs, and of the heart, are located in the midline. The first visible sign of left–right (L–R) asymmetry is the right-sided looping of the developing heart. In amniotes, the second visible asymmetrical event occurs a few hours after heart looping and is called axial rotation or turning. This crucial developmental process consists of a morphogenetic movement at the beginning of which (six to eight somite stage) the embryo's longitudinal axis is curved forming a 'U' with the dorsal side in the concavity. A counter-clockwise twisting of the axis over itself ('axial rotation') changes the dorsal/ventral relation, so that the embryo ends up like a 'U' with the dorsal side in the convexity. Ultimately, all visceral organs show L–R asymmetry, either because they develop as single organs such as the heart, stomach and spleen or because bilateral paired organs such as the lungs display more lobes on one side versus the other. Alterations in the process of L–R specification can lead to severe defects, including L–R reversals of organ position (situs inversus), mirror image symmetry of bilaterally asymmetric tissues (isomerism) and/or random and independent occurrence of laterality defects in different tissues (heterotaxia). The current model of L–R determination hypothesizes a primordial asymmetrical event, which would break L–R symmetry. This would lead to a cascade of laterality decisions mediated by a pathway of regulatory genes acting during gastrulation and early neurulation. The resulting L–R positional information is transferred outward to the lateral plate mesoderm (LPM), where it acts to generate the final position of individual organs (for review, see Harvey, 1998; King et al., 1998; Ramsdell and Yost, 1998; Beddington and Robertson, 1999). Notably, several members of this regulatory pathway are themselves expressed in an L–R asymmetric manner.

Several genes in the L–R pathway have roles that seem evolutionary conserved among vertebrates, including *nodal* (Levin et al., 1995; Collignon et al., 1996; Lowe et al., 1996; Lustig et al., 1996; Lohr et al., 1997; Sampath et al., 1997; Rebagliati et al., 1998a,b) and *lefty2* (Meno et al., 1996, 1997; Bisgrove et al., 1999; Thisse and Thisse, 1999). Both encode distant members of the transforming growth factor β (TGF-β) superfamily, and are asymmetrically expressed in the left LPM. Another conserved asymmetrically expressed gene is the *Pitx2* homeobox gene, perhaps an organ-specific L–R regulator because it is expressed on the left side of many

* Corresponding author. Tel.: +49-551-2011361; fax: +49-551-2011504.

E-mail address: pgruss@gwdg.de (P. Gruss).

0925-4773/02/$ - see front matter
PII: S0925-4773(02)00003-5

tissues (Ryan et al., 1998). In contrast, there are several apparent differences between vertebrate systems that have complicated our understanding of the L–R pathway. For example, many genes displaying transient asymmetry of expression in chicken are not asymmetrically expressed in mouse, including *activin βB*, *activin receptor IIA*, *sonic hedgehog* (*shh*) and fibroblast growth factor 8 (*Fgf8*) (Harvey, 1998; Ramsdell and Yost, 1998; Beddington and Robertson, 1999; Meyers and Martin, 1999). Another unanswered question is the relation between L–R specification and axial rotation, a pivotal event in the development of amniotes. Are both processes interdependent? Which steps of the L–R specification cascade do they share?

In the course of a large-scale gene trap screen (Chowdhury et al., 1997; Bonaldo et al., 1998; Stoykova et al., 1998) we have isolated a novel gene (*rotatin*) coding for a novel protein with three putative transmembrane domains. Mice deficient in this protein cannot complete axial rotation, and show L–R specification alterations. *Rotatin* is a novel player in the L–R specification cascade in the mouse, and represents a genetic link between the processes of axial rotation and those leading to organ asymmetry.

2. Results

2.1. Cloning of rotatin cDNA

In the frame of a large-scale gene trap project carried out on mouse ES cells, we performed a visual screening of embryos in order to identify mutants showing obvious L–R alterations or termination of development around the time of axial rotation/L–R determination. Homozygous embryos originating from ES cell clone XV-53 were selected for further study because they showed obvious alterations of the turning (axial rotation) or the heart looping processes (see below).

Southern blot analyses of genomic DNA from heterozygous animals revealed that one single gene trap vector was integrated into one single site of the genome. Northern blot analysis using the *lacZ* gene as a probe revealed a single band (6.5 kb) (not shown). Subsequently, a 452 bp fragment of the endogenous gene was cloned by 5′ RACE. The sequence of this fragment confirmed correct splicing of the Engrailed-2 splice acceptor to an endogenous splice donor; this resulted in an in-frame fusion of the β-geo coding region with the endogenous gene sequence. The sequence of the trapped gene was searched against databases at the National Center for Biotechnology Information with the BlastN program (Altschul et al., 1990) and similarities were only found to very short expressed sequence tags (ESTs).

Probing murine cDNA libraries with our fragment has yielded so far 5044 bp of cDNA sequence (GenBank Accession Number AF265232) representing the 5′ end of a novel gene that we named *rotatin* (Fig. 1A). The ATG codon at nucleotide positions 259–261 is the strongest candidate for the initiation codon, because it is the starting point of the largest open reading frame (ORF) and there are multiple in-frame stop codons upstream of it. The nucleotides at positions −6, −3 and +4 relative to the ATG correspond to the Kozak motif GCCGCCATGG (Kozak, 1987). The deduced protein (Fig. 1B) comprises 1595 amino acids with a calculated relative molecular mass (M_r) of 178.2 kDa. The integration of the gene trap vector leads to a fusion of the splice donor at nucleotide positions 1101 and 1102 of the *rotatin* cDNA with the splice acceptor of *engrailed-2* exon of the vector. Hence, the insertion predicts the expression of a fusion protein consisting of a severely truncated Rotatin protein (comprising only the first 281 amino acids) and of the β-geo protein (Fig. 1A). Using the Kyte-Doolittle algorithm, three regions with significant hydrophobicity have been found which consequently argue for transmembrane domains (indicated as blocks in Fig. 1C). It is noteworthy that neither similarities to known genes or proteins nor protein motifs have been found in public databases using several programs provided on the Internet. However, a 3.9 kb EST (cr2-00043-a4-z) of rat from the AmGen database has a deduced amino acid sequence with a high degree of sequence conservation with the Rotatin protein. The 3944 bp long rat sequence contains an ORF that could code for a protein 1314 amino acids long. Amino acid sequence comparison showed that both proteins come from homologous or even orthologous genes. The rat EST is about 600 bp 3′ longer than our *rotatin*, and its predicted protein sequence has 196 additional amino acids. Assuming that mouse rotatin possesses, together with the identified 1595 aa, additional 196 aa, the mutant protein contains a maximum of 16% of the wild type protein aa (i.e. 281 of at least 1791 aa).

2.2. Chromosomal localization of the rotatin gene

Low-stringency Southern blot hybridization showed no significant cross-hybridization of the 5′ RACE product with other possible family members. The probe was then used in order to localize the mouse *rotatin* gene in the genome. *Rotatin* was localized close to the telomere of chromosome 18 of the mouse (not shown). This region is homologous to human chromosome 18q. To our knowledge, no human or mouse mutations have yet been mapped to this region.

2.3. Expression pattern of rotatin

We have reported that heterozygous embryos originating from the XV-53 ES cell clone (rotatin) showed β-galactosidase activity in different body regions from E12.5 to E16.5, including the notochord and the central nervous system (Stoykova et al., 1998). We now analyzed earlier embryonic stages and found faint and widespread reporter gene expression in both extraembryonic and embryonic parts of E7.5 heterozygous embryos (Fig. 2A). At E8.5, the most strongly labeled regions included the telencepha-

lon and the mesoderm, particularly the somites (Fig. 2B). We also performed whole mount in situ hybridizations with *rotatin* antisense and sense riboprobes on wild type embryos. At this age, embryos labeled with a riboprobe show staining in the midline, which corresponds to the notochord (Fig. 2C, asterisk). Staining of heterozygous embryos by means of the X-gal reaction (detection of β-galactosidase, the product of the reporter gene *lacZ*) shows light staining of the somites (Fig. 2B), while the *rotatin* riboprobe does not show these mesodermal structures. Together with a very low level of *rotatin* expression in the somites (i.e. a very small amount of *rotatin* transcripts at any given

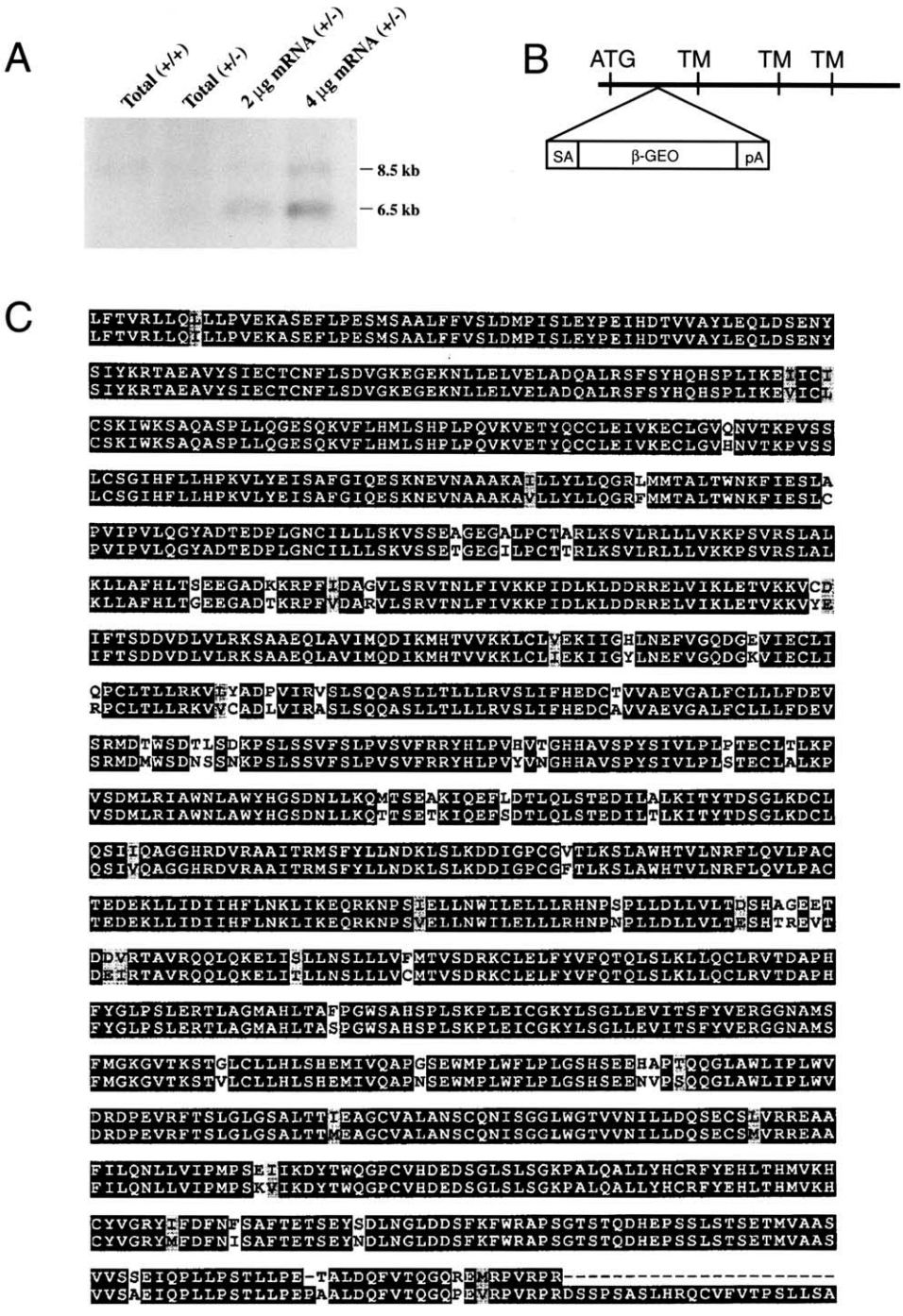

Fig. 1. (A) Northern blot analysis of mRNA from E13.5 embryos wild type or heterozygous for the rotatin^{GT} insertion; wild type embryos show a 6.5 kb transcript; heterozygotes show an additional 8.5 kb band corresponding to the fusion transcript. (B) Insertion site of gene trap vector in the *rotatin* gene; ATG, translation start site; β-geo, *lacZ*-neomycin resistance (neo) fusion; pA, polyadenylation signal; SA, splicing acceptor; TM, predicted transmembrane domain. (C) Comparison between the predicted amino acid sequence of rotatin (upper line) and rat EST cr2-00043-a4-z (lower line); identical amino acids are shown on black background, similar ones on gray.

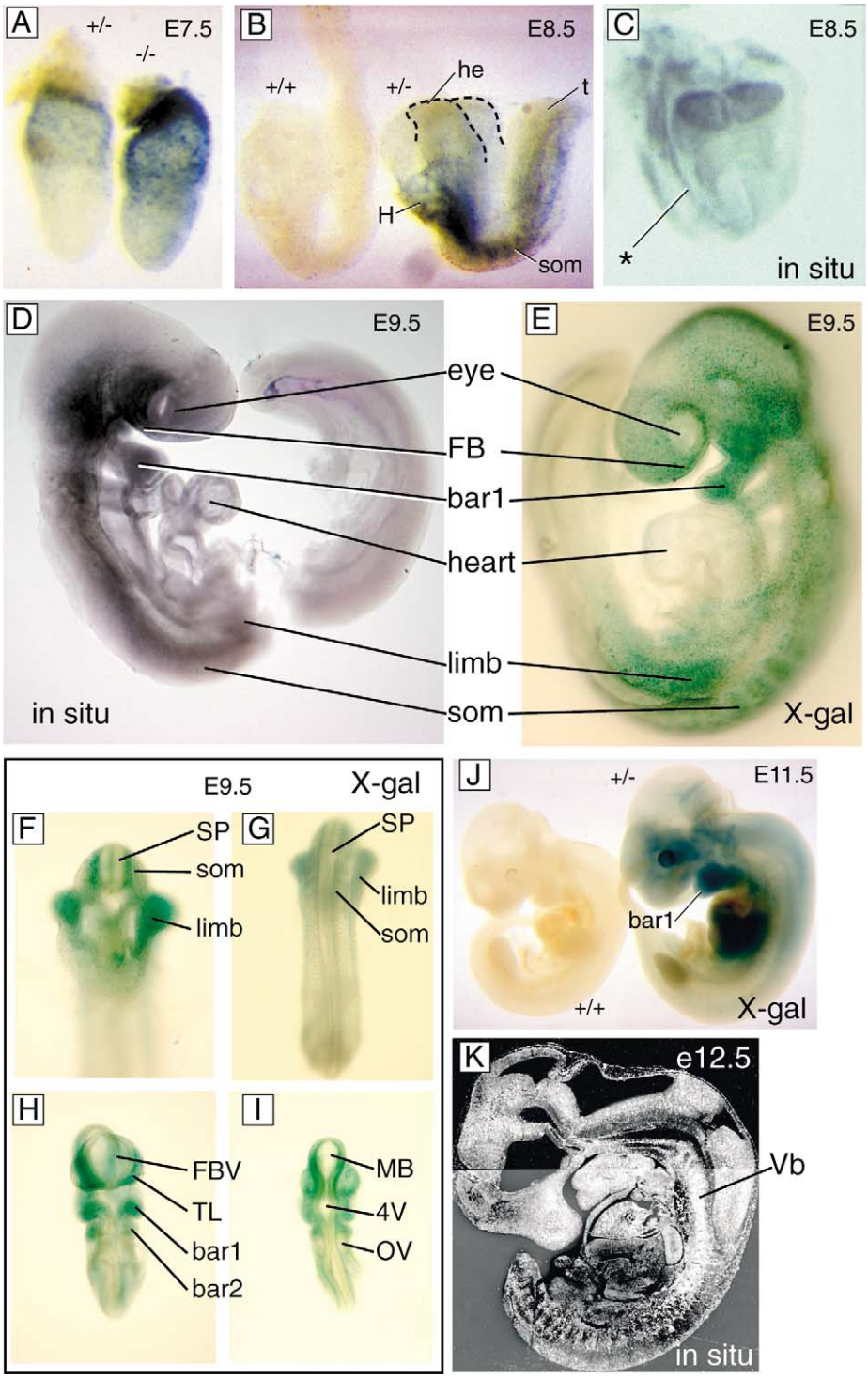

Fig. 2. Expression of *rotatin* in heterozygous embryos. In (A) (E7.5), a homozygous embryo (right) is shown for comparison. (B) By E8.5, the X-gal reaction reveals expression in neural plate and mesodermal derivatives (somites); the heart seems to show some expression too at this age. (C) A somewhat younger embryo labeled by in situ hybridization with a rotatin mRNA probe shows rostral neural plate labeling, as well as putative notochordal labeling (asterisk; see text for details). (D,E) Heterozygous embryos E9.5 labeled by in situ (D) and X-gal reaction (E). Basal forebrain (FB), first branchial arch (bar1) and paraxial mesoderm (somites, som), are labeled in both, as is the forelimb bud. The heart primordium is clearly unlabeled at this age. The caudal half of the embryo in (D) has been cut to make the pattern easier to visualize. (F–I) Views of the caudal (F,G) and rostral (H,I) halves of an X-gal stained heterozygous E9.5 embryo. In (F) and (G) it is clear that the somites, particularly the medial part, as well as the mesoderm of the forelimb bud are labeled. The spinal cord (SP), and the notochordal region ventral to it show only subtle staining. (H,I) The forebrain as well as the midbrain have *rotatin* expression. The first branchial arch and, with less intensity the second, are labeled. (J) By E11.5, the pattern of expression does not change except for that now the heart is labeled. (K) In situ hybridization on sagittal sections shows essentially no change in the expression pattern by E12.5. Abbreviations: 4V, fourth ventricle; bar1, 2, 1st and 2nd branchial arches; FB, forebrain; FBV, forebrain ventricle; H, heart; he, head; limb, forelimb bud; MB, midbrain; som, somites; OV, otic vesicle; SP, spinal cord; t, tail; TL, telencephalon; Vb, vertebrae.

moment), the accumulation of β-galactosidase in the cells over time is a possible explanation of this discrepancy.

By E9.5, the mesodermal expression is still present in the somites, and has started to appear in the forelimb bud (Fig. 2D, E). The basal forebrain and the first branchial arch also show *rotatin* expression. The heart, however, is devoid of expression at this age (Fig. 2D, E). Comparison of X-gal and mRNA detection (in situ hybridization) shows again a discrepancy at the level of the somites (see above). The labeling of midline structures, telencephalon and branchial arches, and the lack of expression by the heart primordium at this age, are coincident in both. We then dissected the bodies of stained embryos in order to examine them in more detail (Fig. 2F–I). Somites and forelimb bud appear labeled as expected (Fig. 2F; dorsal root ganglia are still not present at this age), although staining of the spinal cord and the notochordal region was lighter than expected (Fig. 2F). The caudal part of the embryo (the 'tail') was not labeled (Fig. 2D, E, G). Careful examination of the future facial region and brain confirmed *rotatin* expression in the first and second branchial arches and in the early telencephalic vesicle (Fig. 2H), as well as in the midbrain and hindbrain regions (Fig. 2I). Later in development (E11.5, Fig. 2J; E12.5, Fig. 2K), *rotatin* is expressed in the heart primordium, and the expression in the branchial arches is intensified; the mesodermal expression pattern is maintained (E11.5, Fig. 2J; E12.5, Fig. 2K).

2.4. Rotatin mutants show randomized heart looping

Of 48 offsprings derived from heterozygous parents, 32 animals were heterozygous and were 16 wild type, indicating that rotatin^{GT} homozygotes die before birth. We examined 920 embryos from heterozygous crossings at various gestational ages (Table 1). Embryos showing obvious morphological abnormalities were found around E9.5 and later. All of them were homozygous for the rotatin^{GT} mutation. No homozygous embryos were found beyond E11.5, suggesting that the mutation is lethal around this age. The relative proportions of homozygous, heterozygous and wild type embryos found in our analysis followed the expected Mendelian ratio.

By E9.5, homozygous embryos seemed to be delayed in development as compared to their littermates. The mutants were much smaller (about 50%) than their heterozygous littermates (which show normal phenotype; Fig. 3A, B). The axial rotation was obviously not completed or, in most cases, even started (Fig. 3C–F).

At E10.5, homozygous embryos displayed strong and regular heart beat. Heart development, however, ceased at the looped heart tube stage (see below). A ballooning of the pericardial sac (Fig. 3G) and blood accumulations were found at various regions of freshly dissected homozygous embryos with beating hearts (Fig. 3G). The shape, size and rotation differences between homozygotes and littermates were maintained at this stage (Fig. 3H).

By E11.5, only one-third of the mutants showed beating hearts. The survivors were still smaller than the normal littermates, and had not completed the axial turning (Fig. 3I). At this stage, mutants appeared with left-sided instead of right-sided looping of the heart tube (randomized heart looping; Fig. 3J): 42 of 93 analyzed embryos displayed a reversal in the direction of heart looping (Table 2). The defects in the mutant embryos cannot be attributed to delayed development, since the mutants grow in size and show other developmental processes like closure of the neural tube. At this point, the sum of our results suggested that the XV-53 clone contained a mutation in a novel gene encoding a transmembrane protein whose disruption alters the early developmental processes of heart looping and axial rotation.

2.5. Neural plate and somitic development are altered in rotatin mutants

We decided to characterize the axial rotation defect of the *rotatin* mutants. Turning is a vast morphogenetic event whose mechanism is still unclear. Two embryonic structures have been suggested to be involved, namely the neural tube and the somitic series, both expressing high levels of *rotatin*. The fact that the neural tube grows faster than the underlying endodermal structures has been suggested as a major cause for embryo turning (Jacobson and Tam, 1982; Tam et al., 1982). Other studies point to differential mitotic rates between both sides of the neural tube (Poelmann et al., 1987) as having a role in this process. Involvement of the neural tube in the turning process would also agree with our observation that formation of the neural tube from the neural plate (neurulation) is delayed in rotatin^{GT} embryos (not shown). Consequently, we decided to look at the expression of key neural marker genes in our mutants. Transcription factor *Pax6* is an early marker of the neuroepithelium with

Table 1
Embryonic lethality of the *rotatin* insertional mutation

Age (days)	Totalconceptuses	Wild type	Heterozygous	Homozygous embryos	No. abnormal embryos
E7.5	113	28	62	23	0
E8.5	690	187	327	176	0
E9.5	70	16	33	21	21
E10.5	36	14	13	9	9
E11.5	11	3	5	3	3
Total	920	248 (27%)	440 (48%)	232 (25%)	33

important functions in the differentiation of nuclei at every level of the neural tube (Stoykova et al., 1996; Walther and Gruss, 1991). Its level of expression appeared, in general, to be decreased, and expression was totally absent at caudal levels (Fig. 4A). *Wnt1* and *En1* are early markers of the neuroepithelium of the midbrain–hindbrain junction, and their function is essential for the correct development of this part of the brain (Joyner, 1996). Both of them showed reduced expression intensity as well as loss of expression domains in our mutants (Fig. 4B, C). Therefore, delayed neural tube morphogenesis (neurulation) and altered regionalization–differentiation are hallmarks of the rotating^{GT} phenotype.

Studies on the asymmetric morphogenesis of the somites have pointed out that the formation of these structures probably contributes to turning (Matsuda, 1991). Again this hypothesis agrees with our own observations on the phenotype of rotatin^{GT} embryos. By E9.5, rotatin^{GT} embryos show at most 10–12 somite pairs (wild type embryos have 21–29); in the following hours the somites seem to fuse with each other, and by E10.5 no somitic structure is recognizable in the mutants (not shown). Therefore, we looked at the expression of some regulatory genes playing key roles in somitic development. While expression of *Paraxis*, a transcription factor gene essential for somite morphogenesis (Burgess et al., 1996) is normal in rotatin^{GT} embryos (Fig. 4D), expression of *Pax3* (Goulding et al., 1991) and Delta-like 1 (Dll1) (Bettenhausen et al., 1995), two genes involved in the regulatory pathways of somite differentiation, is altered. In rotatin^{GT} embryos, Pax3 is present in the neural tube but absent from the somites (Fig. 4E) while *Dll* is absent from the normal expressing regions, presomitic mesoderm and posterior half of somites (Fig. 4F).

These results suggested that the cause of the axial rotation failure in rotatin^{GT} mutants were both altered somitic development as well as altered nervous system differentiation and neurulation.

Table 2
Direction of heart looping in homozygous rotatin^{GT} embryos

Age (days)	No. of embryos with right-sided heart looping	No. of embryos with left-sided heart looping	No. of embryos with ventral-sided heart looping
E8.75–9.0	2	2	0
E9.5	41	34	3
E10.5	4	4	0
E11.5	1	2	0
Total	48 (52%)	42 (45%)	3 (3%)

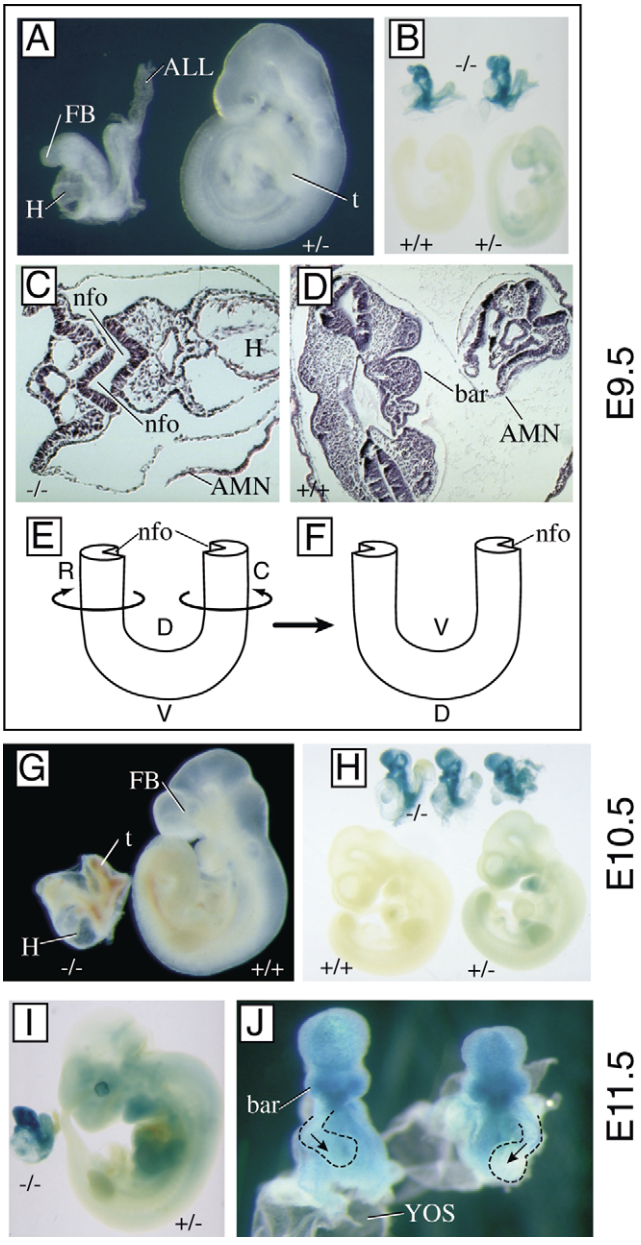

Fig. 3. Heart looping and axial rotation defects in rotatin^{GT} homozygotes. (A) Appearance of homozygotes (left) and heterozygotes (right) at E9.5; (B) β-Galactosidase activity in homozygotes (up) and heterozygotes (down) at E9.5. (C) Cresyl-violet stained section of E9.5 homozygous embryo. The rotation has not taken place: dorsal is still in the concavity, as evidenced by the position of the neural folds (nfo). (D) Cresyl-violet stained section of E9.5 heterozygous embryo. The rotation is taking place (note the position of the neural folds, nfo). (E,F) Diagrams of the axial rotation illustrating the position of the embryos shown in (C,D) respectively; the circular arrows represent the anti-clockwise normal axial rotation; the larger arrow represents the normal sequence of events (after Kaufman, 1990). (G) Appearance of homozygotes (left) and heterozygotes (right) at E10.5. Note the dilated pericardial sac and the abnormal collections of blood in the homozygous. (H) β-Galactosidase activity in homozygotes (up) and heterozygotes (down) at E10.5. (I) Appearance and β-galactosidase activity in E11.5 homozygotes (left) and heterozygotes (right). (J) Front view of E11.5 mutant embryos showing randomized heart looping. Dotted lines delineate heart loop; arrows show looping direction. Abbreviations: ALL, allantois; AMN, amniotic membrane; bar, branchial arch; C, caudal; D, dorsal; FB, forebrain; H, heart; nfo, neural fold; R, rostral; t, tail; V, ventral; YOS, yolk sac.

2.6. The notochord is affected

The notochord is a rod-like embryonic midline structure,

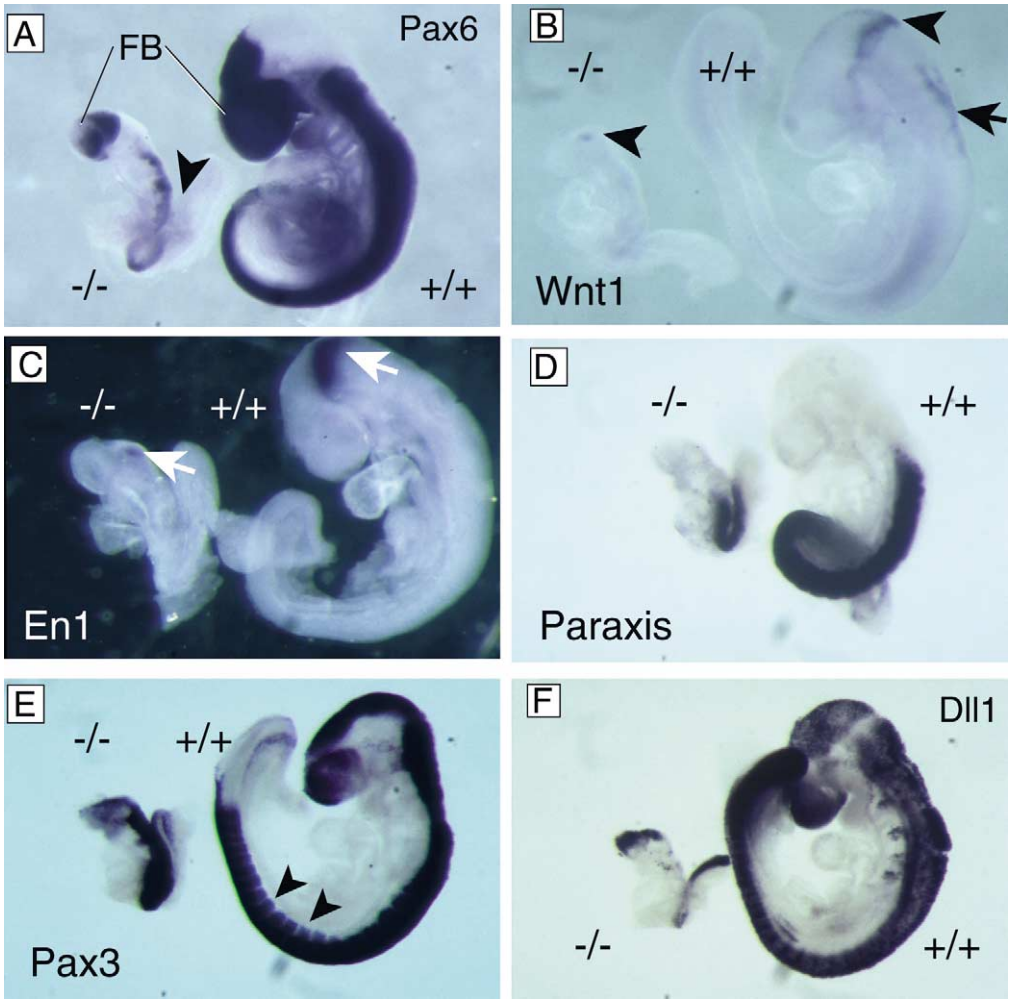

Fig. 4. Expression of CNS markers and somite markers in E9.5 embryos either homozygous (left) or wild type (right) for the rotatin^{GT} insertion. (A) *Pax6* expression intensity was very much reduced in mutant neural tube and completely lost in the caudalmost spinal cord (arrowhead). (B) Mesencephalic expression of *Wnt1* (arrowheads) was conserved in the homozygote, although the rhombencephalic domain (arrow) has disappeared. (C) The mesencephalic domain of *En1* (arrows) was greatly reduced in homozygotes. (D) *Paraxis* expression in the homozygous rostral paraxial mesoderm and already formed somites paralleled wild type expression. (E) *Pax3* was expressed in the homozygous spinal cord, but not in the somitic dermomyotome, which showed expression in the wild type (arrowheads). (F) *Dll1* conserved its head and tail expression domains in the homozygote, but was not expressed in the presomitic mesoderm or the posterior half of the somites, which were labeled in the wild type. Abbreviation: FB, forebrain.

which has an important role in nervous system differentiation (Placzek et al., 1990). Furthermore, rapid elongation of the notochord is one of the causes of neurulation (Jacobson and Gordon, 1976). In addition, the morphological integrity of the notochord is compromised in one naturally occurring mutation (Melloy et al., 1998) whose phenotype resembles that of rotatin^{GT} mutants and also includes turning failure. A morphological comparison of the notochord of wild type and mutant embryos (Fig. 5A, B) on transverse sections revealed gross defects in the mutant. While the wild type notochord shows a compact appearance, in the mutant notochord the cells appeared separated (as opposed to the usual aggregated cell mass), not forming a compact structure, and showing many dense (pyknotic) profiles. These are usually considered as the result of the destruction of the cell nucleus, which is a consequence of cell death processes (see box in Fig. 5B). Consequently, we examined expression of genes known to be important in notochord formation and/or maintenance. *shh* (Echelard et al., 1993), *HNF3β* (Ang et al., 1993) and *bra* (Herrmann et al., 1990) are genes reported to be essential for the proper development of the notochord. *shh*, which also has a major role in L–R specification (Harvey, 1998), is absent from the rostral half of the notochord of rotatin^{GT} embryos (Fig. 5C). *HNF3β* (Ang et al., 1993), essential for proper notochordal development, is absent from this structure (not shown) and also from the neural plate (Fig. 5D). *bra* expression was already abnormal in homozygous *rotatin* embryos having two to four somites, in that the normally compact and rod-like expression was fragmented and showed signs of degeneration (Fig. 5E). At this point, our results suggested that morphological and functional alterations of the notochord could be at the root of the axial rotation failure in our mutants.

2.7. Alteration of the L–R specification cascade in rotatin mutants

The notochord has been reported to be crucial not only for turning but also for L–R specification (Danos and Yost, 1996; King et al., 1998; Melloy et al., 1998). That this process could be altered in our mutants was suggested by the randomization of heart looping that they present. We

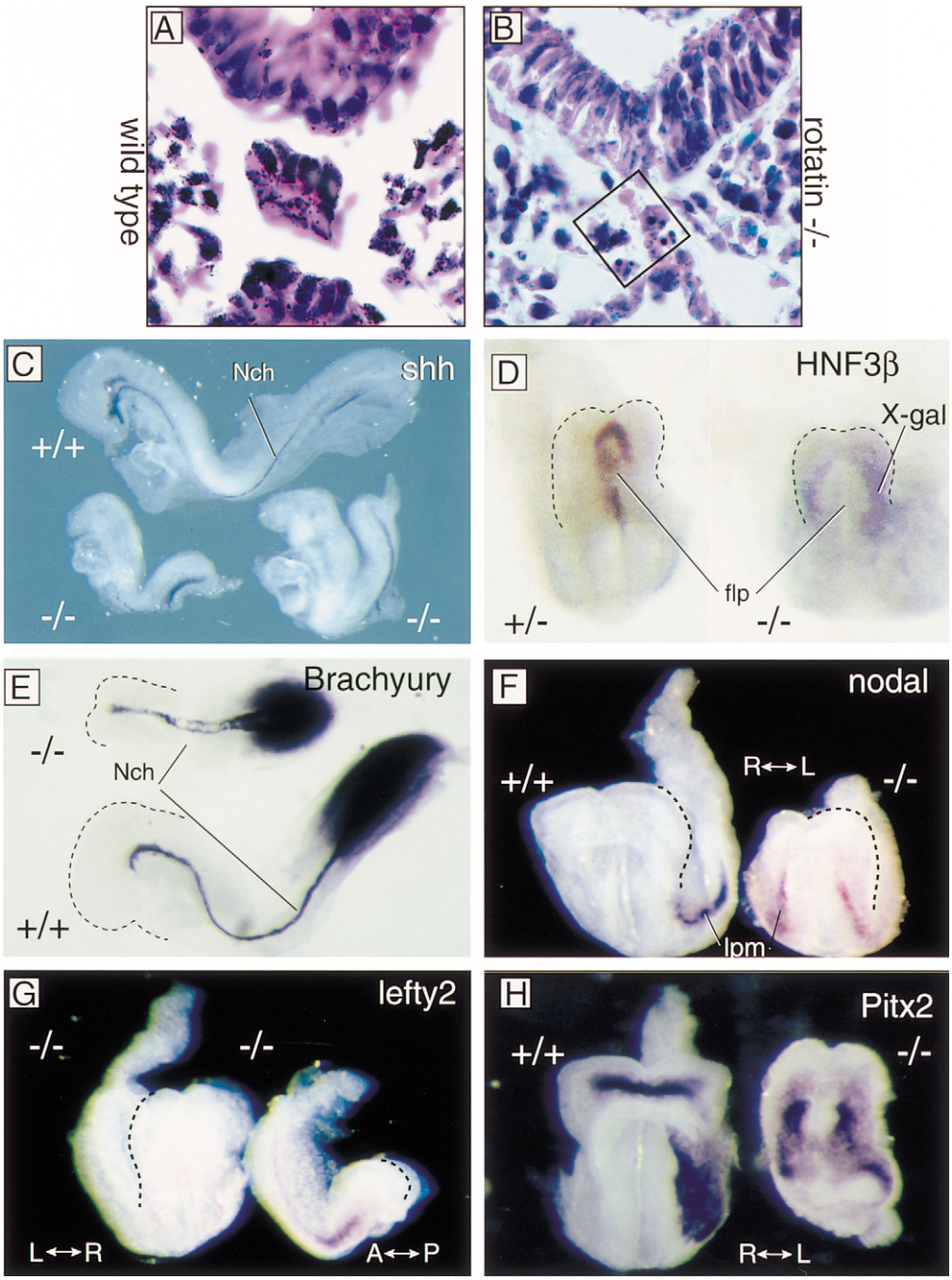

Fig. 5. Expression of notochord markers and L–R markers in E8.5 embryos either homozygous or wild type for the rotatin^{GT} insertion. (A,B) Wild type (A) and rotatin^{GT} homozygous (B) notochords, in transversal sections stained with hematoxylin–eosin. The box in (B) marks the normal position of the notochord; the notochordal cells are abnormally separated, and abundant pyknotic nuclei can be seen (cell death). (C) Expression of *shh* in wild type notochord (upper) contrasts with the expression only in the caudal half of mutant notochord (lower). (D) *HNF-3β* is present at this age in the heterozygote (left), but absent in the homozygote (right; this homozygous embryo is also stained for β-galactosidase expression by the X-gal reaction). (E) *bra* expression in wild type notochord is a compact cordon (lower); in homozygotes, expression is maintained, but the notochord shows a 'hollow' appearance (upper). (F) *nodal* expression in the lateral mesoderm appears only in the left side in wild type embryos (left), but on both sides of the homozygote (right). (G) Homozygotes showing *lefty2* expression on the right side (right) or not at all (left). (H) Expression of *Pitx2* is lateralized in wild type (left), but not in homozygotes (right). Abbreviations: lpm, lateral plate mesoderm; flp, floor plate; Nch, notochord.

decided to analyze the workings of this mechanism in these embryos. A current model for L–R specification (Harvey, 1998) postulates a crucial role for *shh* as key intermediate between a primordial asymmetric event (which would take place in the midline) and the downstream carriers of laterality information to the organs (which act in the LPM). Expression of *shh* was altered in our mutants in such a way that the rostral half of the notochord was completely devoid of transcripts (Fig. 5C).

Accordingly, we then checked the mutant expression of the next members of the lateralization cascade. Genes *nodal* (Zhou et al., 1993) and *lefty2* (Meno et al., 1997) are two TGF-β superfamily members currently considered as good candidates to relay the L–R information from *shh* to the LPM. Both are normally expressed transiently at the two to six somite stage in the left LPM before morphological asymmetries such as the heart looping become evident. *nodal* is normally expressed in the left LPM and around the node (Fig. 5F, left). In rotatin^{GT} embryos, asymmetric *nodal* expression at the node was retained, but was detected in both the left and right LPM (Fig. 5F, right). *Lefty-2* is active in the left LPM and also, weakly, in the floor plate of the neural tube (Meno et al., 1996, 1997). *Lefty-2* expression was dramatically changed in rotatin^{GT} embryos. Expression was either bilateral (Fig. 5G, left) or absent (Fig. 5G, right). The homeobox-containing gene *Pitx2* is asymmetrically expressed in the LPM and in the asymmetrically developing organs as well (St. Amand et al., 1998). *Pitx2* is downstream *nodal* (Logan et al., 1998) and seems to be at the end of the cascade of lateralization: it delivers the L–R information to the organs (Levin et al., 1997). Half of the analyzed rotatin^{GT} embryos showed no *Pitx2* expression and the other half displayed expression on both body sides (Fig. 5H, right). Interestingly, no homozygous embryo exhibited *Pitx2* transcriptional activity in the head mesenchyme, which is the case for wild type embryos (Fig. 5H, left).

In order to position *rotatin* with more precision in the chain of events leading to laterality, we wanted to check the expression of genes crucial for this process but which find themselves upstream nodal. L–R dynein (lrd) is a microtubule-based motor whose deficiency causes abnormal expression of *nodal* and *lefty2* in the mouse embryo, leading finally to situs inversus (Supp et al., 1997, 1999). Our RT-PCR experiments (Fig. 6A) show that *lrd* is expressed in rotatin^{GT} homozygotes. Deficiency in the protein inversin is also the cause of *nodal* and *lefty2* expression alterations which end up in situs inversus (Mochizuki et al., 1998; Morgan et al., 1998). RT-PCR shows that *inversin* is also expressed in our mutants (Fig. 6B). The expression of *rotatin* and that of *lrd* and *inv* are too subtle and widespread to determine by in situ hybridization if they could be downregulated in some specific region in our mutants. The possibility still exists that one of these genes, or both, is downregulated in a subtle way in our mutants, in some of the ample territories of expression that they share with *rotatin*.

Therefore, deficiency in *rotatin* causes a morphological

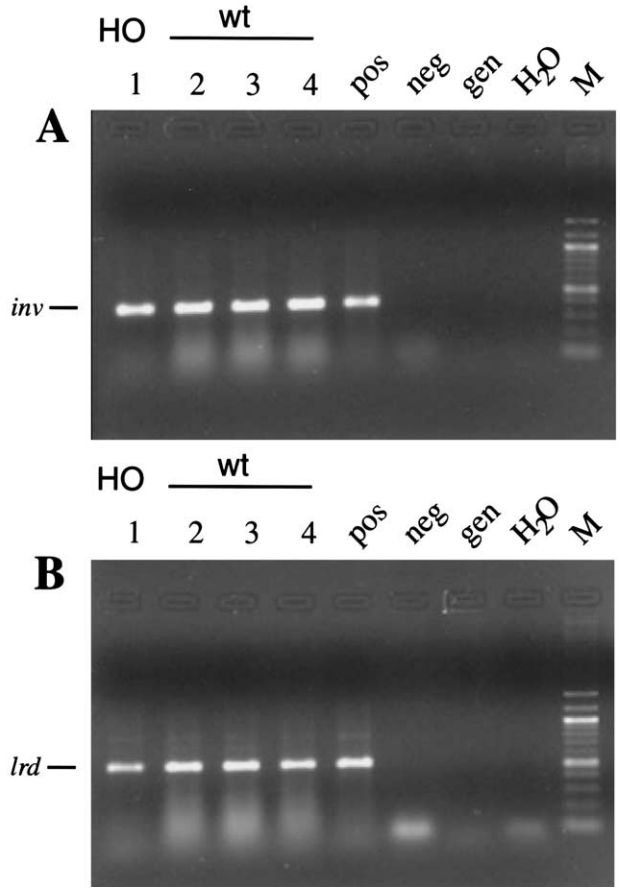

Fig. 6. RT-PCR demonstrates the presence of *inversin* (*inv*, panel A) and *L–R dynein* (*lrd*, panel B) in rotatin^{GT} homozygotes. HO, homozygous total RNA; wt, wild type total RNA of littermates; pos, total RNA from non-related wild type mouse; neg, PCR without reverse transcription; gen, RT-PCR using genomic DNA as template; H_2O, RT-PCR using water as template.

and functional alteration of the notochord (also involved in turning failure), which through the consequent alteration of *shh* expression, cascades down the LPM and ends up altering heart looping (i.e. visceral positioning).

3. Discussion

This study shows that *rotatin*, a novel gene, is involved in L–R specification as well as embryo turning, probably through its essential role in notochordal development. Embryos deficient in *rotatin* suffer major developmental defects. These include notochordal degeneration, imperfect differentiation of somites and neural tube, axial rotation failure and randomized heart looping. These embryos die around E11.5.

Genes crucial for notochordal development (*HNF-3β*, *bra*) show altered expression or abnormally absent expression in the mutants, while genes involved in the last part of the lateralization cascade (*nodal*, *lefty2*, *Pitx2*) show bilateral or absent expression (as opposed to the usual asym-

metric expression). Transcripts of *shh*, a gene believed to represent the link between midline structures (notochord) and LPM in the genetic cascade that leads to L–R specification, are abnormally absent in the rostral half of the mutant notochord. Finally, other genes (*inv* and *lrd*) whose deficiency also perturbs the expression of *nodal*, *lefty2* and *Pitx2*, and culminates in a situs inversus phenotype, are still expressed in rotatin^{GT} homozygotes.

3.1. Novel gene rotatin is essential for axial rotation

By the six to eight somite stage, the mouse embryo longitudinal axis is curved forming a 'U' with the dorsal side in the concavity. At this age, a morphogenetic movement starts consisting of a twisting of the axis over itself ('axial rotation'), and resulting in a change in the dorsal/ventral relation, so that the embryo ends up like a 'U' with the dorsal side in the convexity (the 'fetal position'). This process is termed turning or axial rotation and has already been classically described in the 19th century and in the beginning of the 20th century (reviewed in Fujinaga et al., 1995). Recent detailed descriptions (Kaufman, 1990, 1992) describe turning as a counter-clockwise rotation. Fujinaga et al. (1995) have added further details and ultimate refinement to that morphological analysis. Although at least some birds and reptiles show 90 degree turning (reviewed in Poelmann et al., 1987), 180 degree turning appears only in mammals. Even in this class, turning appears only in some species, and can be considered something of a rarity. In the evolution of gastrulation, axial rotation can be considered as an outgrowth of the L–R specification mechanism which was selected because it represents the way out for a process that would otherwise end up as a developmental cul de sac, e.g. the so-called 'cylinder egg'. Among the species which develop by means of cylinder eggs are some favorite models like mouse, rat, rabbit and guinea pig (Snell, 1941), but not human.

Embryos deficient in *rotatin* do not perform axial rotation, although some show indications of having started the process. One possible explanation could be that deficiency in *rotatin* blocks development at a stage prior to turning. However, although rotatin^{GT} homozygotes are not able to turn, they keep growing until E11.5 (Fig. 4). In the absence of turning, heart development cannot progress correctly. The 'cylinder egg position' (as opposed to the 'fetal position', where dorsal is in the convexity) prevents closure of the body walls, endoderm differentiation and ultimately, organogenesis. These problems, together with the accompanying differentiation defects in neural tube and somites, could cause the lethality of the rotatin^{GT} mutation.

3.2. Rotatin in the L–R regulatory cascade

The earliest visible effect of L–R specification is the anticlockwise turning of the longitudinal embryo axis as revealed first by the looping of the heart primordium towards the right. Mutants with turning failure show altered visceral asymmetry or altered expression of *nodal*, *lefty2* and *Pitx2* (this is the case for instance of the 'no turning' natural mutation) (Melloy et al., 1998), the *furin* null mutation (Roebroek et al., 1998; Constam and Robertson, 2000) and the rotatin^{GT} mutation. However, mutants can show altered visceral asymmetry while undergoing correct turning (this is the case, for instance, of fused toes) (Heymer et al., 1997), situs inversus viscerum and inversion of embryonic turning (Lowe et al., 1996) and SIL-deficient mutants (Izraeli et al., 1999). Therefore, the process of turning cannot be independently affected by mutation, although it can be spared by mutations of later genes. This suggests that at an early phase the control mechanisms for turning and for visceral L–R specification share crucial components, then separate into distinct regulatory cascades. According to our data, rotatin is not required to put in place the notochord, but it is essential to maintain its morphology and function, at least in part by contributing to maintaining the expression of *HNF-3β*.

Inv and *lrd* are non-asymmetrically expressed genes involved in L–R specification. The fact that mutation of these genes causes visceral asymmetry alteration (Lowe et al., 1996; Supp et al., 1997; Mochizuki et al., 1998; Morgan et al., 1998) but not turning failure places them functionally downstream rotatin. Both *inv* and *lrd* are, however, expressed in our mutants (Fig. 7), suggesting that the L–R specification does not depend on a linear cascade but on a network of regulatory processes where different and relatively independent parts have to act in cue. The importance of timing and the complexity of the interactions relevant to L–R specification have been emphasized by Izraeli et al. (1999).

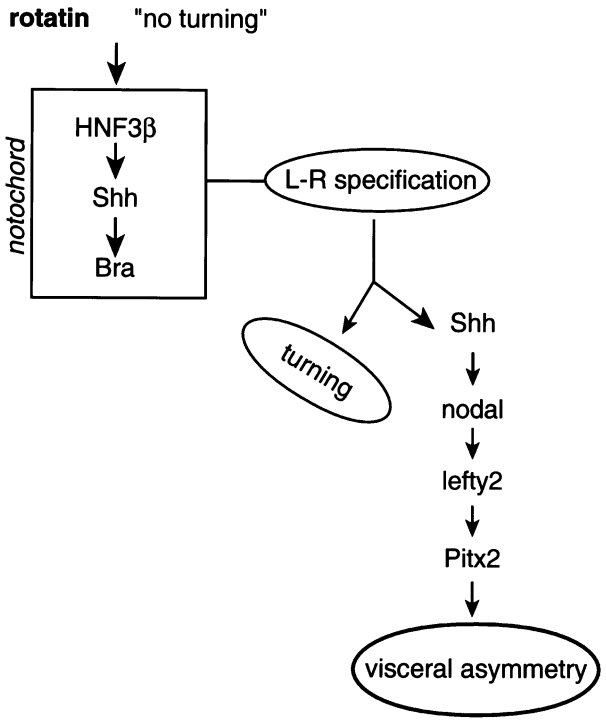

Fig. 7. Diagram showing the possible position of rotatin in the genetic cascades for axial rotation and visceral asymmetry.

In summary, L–R specification starts in the midline (node), progresses through the axial midline (notochord) and is finally communicated to the sides (LPM) where the actual organogenesis takes place. The notochordal alterations present in rotatin^{GT} mutants, together with the alteration in the expression of midline gene *shh* as well as LPM genes *nodal*, *lefty* and *Pitx2*, place *rotatin* as a midline gene linking the processes of asymmetric visceral development and axial rotation through its essential role in the maintenance of the notochord.

3.3. Axial rotation and the notochord

Within the midline, the notochord seems to be a crucial structure for both axial rotation and visceral asymmetry specification (Bisgrove et al., 2000). Asymmetric expression of *lefty1* on the left side of the midline depends not only on the initiating signals from the node, but also on the integrity of the midline and on the activity of genes (*shh*, *bra*, *HNF-3β*) expressed by midline cells (reviewed in Capdevila et al., 2000). Besides, experiments in *Xenopus* and zebrafish have shown the notochord to be essential for the coordination of the body axes (Danos and Yost, 1996). Finally, in both the 'no turning' mutants (Melloy et al., 1998) and the rotatin^{GT} mutants analyzed in this study, failure of axial rotation correlates with notochord degeneration.

The notochord can presumably exert direct and indirect influence on rotation. Because it is a compact bar of cells spanning the length of the embryo, the notochord has large morphogenetic potential (Keller et al., 2000), and could represent a hard core around which the embryo can revolve. Its physical integrity would then be of major importance for this process. The notochord has also a crucial role in the differentiation of structures reported to be involved in the mechanism of turning. Differential mitotic rates in the neural tube (Poelmann et al., 1987) and rapid growth of the neural tube (Jacobson and Tam, 1982; Tam et al., 1982) as well as somite morphogenesis (Matsuda, 1991) have been shown to be among the causes of axial rotation. The notochord is known to be essential for the differentiation of the neural tube (Placzek et al., 1990). In addition, both notochord and neural tube have a central role in somitic differentiation (for review see Brand-Saberi and Christ, 2000; Dockter, 2000; Holley and Nusslein-Volhard, 2000). Rotatin mutants show not only notochord degeneration, but gross alteration of neural and somitic differentiation as well. One of these factors or more probably a combination thereof is very likely to be responsible for the turning defect.

3.4. The rotatin^{GT} phenotype matches that of 'no turning'

One of the most interesting phenotypes showing axial rotation failure is due to a spontaneous mouse recessive mutation which has been named 'no turning' (Melloy et al., 1998). The reported phenotype of 'no turning' mutants is strikingly similar to the one of rotatin^{GT} mice as described in the present study. It seems very likely that *rotatin* is functionally very closely related to the gene mutated in 'no turning'. It is also conceivable that rotatin^{GT} and 'no turning' affect the same gene. Melloy et al. (1998) conclude their paper making a good case for the involvement of 'no turning' in the modulation of *HNF-3β* expression in the notochord. They also suggest that the level of notochordal expression of *HNF-3β* is critical to the establishment of L–R determination. If *rotatin* is indeed the gene mutated in 'no turning', pursuing research in these intriguing developments would be greatly facilitated.

4. Materials and methods

4.1. Derivation of mutant mice and cloning of rotatin cDNA

The generation of rotatin^{GT} mice by morula aggregation of embryonic stem (ES) cell line XV-53 containing an insertion of the gene trap vector pGT1.8geo (Skarnes et al., 1995) has been described previously (Stoykova et al., 1998). The 5′ RACE on RNA of an embryonic day 13.5 (E13.5) embryo and an adult brain isolated by Trizol (Gibco) yielded 452 bp of endogenous and around 200 bp of vector sequences. A fragment devoid of vector sequences was used to screen an E14.5 mouse cDNA library (Wijnholds et al., 1995) yielding several overlapping clones that were sequenced. A consensus fragment, 5044 bp long, was obtained, which potentially codes for a protein of at least 1595 amino acids.

4.2. Northern analyses

Total RNA, 18 μg, and 2 and 4 μg of mRNA isolated from E13.5 wild type and heterozygous embryos were separated in a denaturing 1% agarose gel (containing formaldehyde). After staining with ethidium bromide to confirm the integrity of the RNA, the RNA was transferred to an uncharged nylon membrane (Qiagen). The probe used for hybridization was the 5′ RACE fragment devoid of vector sequence. The hybridization buffer was a modification of the buffer described by Church and Gilbert (1984) in that it contained only 0.5 M $NaHPO_4$, pH 7.2 and 7% SDS. Hybridization and washes (40 mM $NaHPO_4$, pH 7.2, 1% SDS) were done at 65°C.

4.3. Genotyping of mice and embryos

Southern blot analyses of genomic DNA isolated from tail biopsies and embryonic yolk sacs were performed to identify *lacZ* gene carriers. Mice homozygous for the *rotatin* gene trap vector insertion were produced by intercrosses of heterozygous parents. The genotypes of their offspring at weaning stage were determined by quantitative Southern blot analyses on genomic DNA digested with BamH1 and hybridized with both a 3 kb *lacZ* fragment and, as an internal standard, with a 1.3 kb genomic fragment of the *Fkh5* gene (Wehr et al., 1997). The relative intensities of the

bands on the autoradiographs serve to distinguish heterozygous from homozygous mice (Faisst and Gruss, 1998).

The genotype of E6.5–E8.5 embryos was determined by polymerase chain reaction (PCR) or X-gal staining. For PCR genotyping, two pairs of oligonucleotides are needed to distinguish all three genotypes. One pair that recognizes the neomycin resistance gene (BM101 and BM102) and another pair (AF80 and AF82) which flanks the vector integration site were used. For designing the latter oligonucleotides the vector integration site was mapped. Briefly, several restriction fragment length polymorphisms (RFLPs) were identified on genomic DNA using the 5′ RACE product as a probe demonstrating that the vector was integrated 5′ to those restriction sites presumably into an intron. The intron that follows the 5′ RACE exon sequences was sequenced after isolating genomic phages and these restriction sites were identified. Because there was no RFLP found using NdeI or PstI and further Southern blot analyses using intron probes were done, it is very likely that the integration occurred within 72 bp between restriction sites PstI and SpHI. Therefore, the primer pair AF80 and AF82 amplifies a 600 bp fragment only of the wild type allele of the *rt* gene and not of the trapped allele because the length is too great for PCR.

X-gal staining represents another reliable way of genotyping with several advantages. It is fast, whole litters can be processed simultaneously and the specimens can be used for in situ hybridization afterwards (Tajbakhsh and Houzelstein, 1995). For that purpose, the embryos were fixed up to 4 h in 4% paraformaldehyde, washed in phosphate buffered saline (PBS), incubated in X-gal or Red-gal (red color) overnight as described by Faisst and Gruss (1998) and then used in standard procedures for whole mount in situ hybridization experiments.

4.4. In situ hybridization and histological analysis

Whole mount in situ hybridization protocols followed standard procedures. Antisense and sense single-stranded RNA probes of the *rt* gene were synthesized using a phagemid clone containing 1 kb of the 5′ end of the cDNA. The phagemid was linearized with BamHI and transcribed with T7 polymerase in the presence of 35-S UTP and 35-S CTP to give the antisense probe, linearized with XhoI and transcribed with T3 polymerase to obtain the sense probe. Probe synthesis, preparation of paraffin sections and hybridization were done as described (Kessel and Gruss, 1991). Probes for the following mouse genes were used: *Pitx2*, *nodal*, *lefty2*, *Brachyury* (*bra*), *shh* and *HNF-3β*.

Acknowledgements

Paolo Bonaldo, Kamal Chowdhury, Anastassia Stoykova and Miguel Torres made this gene trap line available. Juan Carlos Izpisùa Belmonte, Hiroshi Hamada, Bernhard Herrmann, Michael Kuehn and Janet Rossant donated probes. Xunlei Zhou offered valuable comment on the manuscript.

References

Altschul, S.F., Gish, W., Miller, W., Myers, E.W., Lipman, D.J., 1990. Basic local alignment search tool. J. Mol. Biol. 215, 403–410.

Ang, S.L., Wierda, A., Wong, D., Stevens, K.A., Cascio, S., Rossant, J., Zaret, K.S., 1993. The formation and maintenance of the definitive endoderm lineage in the mouse: involvement of HNF3/forkhead proteins. Development 119, 1301–1315.

Beddington, R.S., Robertson, E.J., 1999. Axis development and early asymmetry in mammals. Cell 96, 195–209.

Bettenhausen, B., Hrabe de Angelis, M., Simon, D., Guenet, J.L., Gossler, A., 1995. Transient and restricted expression during mouse embryogenesis of Dll1, a murine gene closely related to *Drosophila* Delta. Development 121, 2407–2418.

Bisgrove, B.W., Essner, J.J., Yost, H.J., 1999. Regulation of midline development by antagonism of lefty and nodal signaling. Development 126, 3253–3262.

Bisgrove, B.W., Essner, J.J., Yost, H.J., 2000. Multiple pathways in the midline regulate concordant brain, heart and gut left–right asymmetry. Development 127, 3567–3579.

Bonaldo, P., Chowdhury, K., Stoykova, A., Torres, M., Gruss, P., 1998. Efficient gene trap screening for novel developmental genes using IRES beta geo vector and in vitro preselection. Exp. Cell Res. 244, 125–136.

Brand-Saberi, B., Christ, B., 2000. Evolution and development of distinct cell lineages derived from somites. Curr. Top. Dev. Biol. 48, 1–42.

Burgess, R., Rawls, A., Brown, D., Bradley, A., Olson, E.N., 1996. Requirement of the paraxis gene for somite formation and musculoskeletal patterning. Nature 384, 570–573.

Capdevila, J., Vogan, K.J., Tabin, C.J., Izpisua Belmonte, J.C., 2000. Mechanisms of left–right determination in vertebrates. Cell 101, 9–21.

Chowdhury, K., Bonaldo, P., Torres, M., Stoykova, A., Gruss, P., 1997. Evidence for the stochastic integration of gene trap vectors into the mouse germline. Nucleic Acids Res. 25, 1531–1536.

Church, G.M., Gilbert, W., 1984. Genomic sequencing. Proc. Natl Acad. Sci. USA 81, 1991–1995.

Collignon, J., Varlet, I., Robertson, E.J., 1996. Relationship between asymmetric nodal expression and the direction of embryonic turning. Nature 381, 155–158.

Constam, D.B., Robertson, E.J., 2000. Tissue-specific requirements for the proprotein convertase furin/SPC1 during embryonic turning and heart looping. Development 127, 245–254.

Danos, M.C., Yost, H.J., 1996. Role of notochord in specification of cardiac left–right orientation in zebrafish and *Xenopus*. Dev. Biol. 177, 96–103.

Dockter, J.L., 2000. Sclerotome induction and differentiation. Curr. Top. Dev. Biol. 48, 77–127.

Echelard, Y., Epstein, D.J., St.-Jacques, B., Shen, L., Mohler, J., McMahon, J.A., McMahon, A.P., 1993. Sonic hedgehog, a member of a family of putative signaling molecules, is implicated in the regulation of CNS polarity. Cell 75, 1417–1430.

Faisst, A.M., Gruss, P., 1998. Bodenin: a novel murine gene expressed in restricted areas of the brain. Dev. Dyn. 212, 293–303.

Fujinaga, M., Hoffman, B.B., Baden, J.M., 1995. Axial rotation in rat embryos: morphological analysis and microsurgical study on the role of the allantois. Teratology 51, 94–106.

Goulding, M.D., Chalepakis, G., Deutsch, U., Erselius, J.R., Gruss, P., 1991. Pax-3, a novel murine DNA binding protein expressed during early neurogenesis. EMBO J. 10, 1135–1147.

Harvey, R.P., 1998. Links in the left/right axial pathway. Cell 94, 273–276.

Herrmann, B.G., Labeit, S., Poustka, A., King, T.R., Lehrach, H., 1990. Cloning of the T gene required in mesoderm formation in the mouse. Nature 343, 617–622.

Heymer, J., Kuehn, M., Ruther, U., 1997. The expression pattern of nodal

and lefty in the mouse mutant Ft suggests a function in the establishment of handedness. Mech. Dev. 66, 5–11.
Holley, S.A., Nusslein-Volhard, C., 2000. Somitogenesis in zebrafish. Curr. Top. Dev. Biol. 47, 247–277.
Izraeli, S., Lowe, L.A., Bertness, V.L., Good, D.J., Dorward, D.W., Kirsch, I.R., Kuehn, M.R., 1999. The SIL gene is required for mouse embryonic axial development and left–right specification. Nature 399, 691–694.
Jacobson, A.G., Gordon, R., 1976. Changes in the shape of the developing vertebrate nervous system analyzed experimentally, mathematically and by computer simulation. J. Exp. Zool. 197, 191–246.
Jacobson, A.G., Tam, P.P., 1982. Cephalic neurulation in the mouse embryo analyzed by SEM and morphometry. Anat. Rec. 203, 375–396.
Joyner, A.L., 1996. Engrailed, Wnt and Pax genes regulate midbrain–hindbrain development. Trends Genet. 12, 15–20.
Kaufman, M.H., 1990. Morphological stages of postimplantation embryonic development. Copp, A.J., Cockroft, D.L. (Eds.), Postimplantation Mammalian Embryos. A Practical Approach, IRL Press, Oxford, pp. 81–91.
Kaufman, M.H., 1992. The Atlas of Mouse Development, Academic Press, London.
Keller, R., Davidson, L., Edlund, A., Elul, T., Ezin, M., Shook, D., Skoglund, P., 2000. Mechanisms of convergence and extension by cell intercalation. Philos. Trans. R. Soc. Lond. B Biol. Sci. 355, 897–922.
Kessel, M., Gruss, P., 1991. Homeotic transformations of murine vertebrae and concomitant alteration of Hox codes induced by retinoic acid. Cell 67, 89–104.
King, T., Beddington, R.S., Brown, N.A., 1998. The role of the brachyury gene in heart development and left–right specification in the mouse. Mech. Dev. 79, 29–37.
Kozak, M., 1987. An analysis of 5′-noncoding sequences from 699 vertebrate messenger RNAs. Nucleic Acids Res. 15, 8125–8148.
Levin, M., Johnson, R.L., Stern, C.D., Kuehn, M., Tabin, C., 1995. A molecular pathway determining left–right asymmetry in chick embryogenesis. Cell 82, 803–814.
Levin, M., Pagan, S., Roberts, D.J., Cooke, J., Kuehn, M.R., Tabin, C.J., 1997. Left/right patterning signals and the independent regulation of different aspects of situs in the chick embryo. Dev. Biol. 189, 57–67.
Logan, M., Pagan-Westphal, S.M., Smith, D.M., Paganessi, L., Tabin, C.J., 1998. The transcription factor Pitx2 mediates situs-specific morphogenesis in response to left–right asymmetric signals. Cell 94, 307–317.
Lohr, J.L., Danos, M.C., Yost, H.J., 1997. Left–right asymmetry of a nodaL–Related gene is regulated by dorsoanterior midline structures during *Xenopus* development. Development 124, 1465–1472.
Lowe, L.A., Supp, D.M., Sampath, K., Yokoyama, T., Wright, C.V., Potter, S.S., Overbeek, P., Kuehn, M.R., 1996. Conserved left–right asymmetry of nodal expression and alterations in murine situs inversus. Nature 381, 158–161.
Lustig, K.D., Kroll, K., Sun, E., Ramos, R., Elmendorf, H., Kirschner, M.W., 1996. A *Xenopus* nodaL–Related gene that acts in synergy with noggin to induce complete secondary axis and notochord formation. Development 122, 3275–3282.
Matsuda, M., 1991. Change of rat embryos from a ventrally concave U-shape to a ventrally convex C-shape. Dev. Growth Differ 33, 117–122.
Melloy, P.G., Ewart, J.L., Cohen, M.F., Desmond, M.E., Kuehn, M.R., Lo, C.W., 1998. No turning, a mouse mutation causing left–right and axial patterning defects. Dev. Biol. 193, 77–89.
Meno, C., Saijoh, Y., Fujii, H., Ikeda, M., Yokoyama, T., Yokoyama, M., Toyoda, Y., Hamada, H., 1996. Left–right asymmetric expression of the TGF beta-family member lefty in mouse embryos. Nature 381, 151–155.
Meno, C., Ito, Y., Saijoh, Y., Matsuda, Y., Tashiro, K., Kuhara, S., Hamada, H., 1997. Two closely-related left–right asymmetrically expressed genes, lefty-1 and lefty-2: their distinct expression domains, chromosomal linkage and direct neuralizing activity in *Xenopus* embryos. Genes. Cells 2, 513–524.
Meyers, E.N., Martin, G.R., 1999. Difference in left–right axis pathways in mouse and chick: functions of FGF8 and SHH. Science 285, 403–406.
Mochizuki, T., Saijoh, Y., Tsuchiya, K., Shirayoshi, Y., Takai, S., Taya, C., Yonekawa, H., Yamada, K., Nihei, H., Nakatsuji, N., Overbeek, P.A., Hamada, H., Yokoyama, T., 1998. Cloning of inv, a gene that controls left/right asymmetry and kidney development. Nature 395, 177–181.
Morgan, D., Turnpenny, L., Goodship, J., Dai, W., Majumder, K., Matthews, L., Gardner, A., Schuster, G., Vien, L., Harrison, W., Elder, F.F.B., Penman-Splitt, M., Overbeek, P., Strachan, T., 1998. Inversin, a novel gene in the vertebrate left–right axis pathway, is partially deleted in the inv mouse. Nat. Genet. 20, 149–156.
Placzek, M., Tessier-Lavigne, M., Yamada, T., Jessell, T., Dodd, J., 1990. Mesodermal control of neural cell identity: floor plate induction by the notochord. Science 250, 985–988.
Poelmann, R.E., Mentink, M.M., van Leeuwen, J.L., 1987. Axial rotation of murine embryos, a study of asymmetric mitotic activity in the neural tube of somite stages. Anat. Embryol. 176, 99–103.
Ramsdell, A.F., Yost, H.J., 1998. Molecular mechanisms of vertebrate left–right development. Trends Genet. 14, 459–465.
Rebagliati, M.R., Toyama, R., Fricke, C., Haffter, P., Dawid, I.B., 1998a. Zebrafish nodaL–Related genes are implicated in axial patterning and establishing left–right asymmetry. Dev. Biol. 199, 261–272.
Rebagliati, M.R., Toyama, R., Haffter, P., Dawid, I.B., 1998b. Cyclops encodes a nodaL–Related factor involved in midline signaling. Proc. Natl Acad. Sci. USA 95, 9932–9937.
Roebroek, A.J., Umans, L., Pauli, I.G., Robertson, E.J., van Leuven, F., Van de Ven, W.J., Constam, D.B., 1998. Failure of ventral closure and axial rotation in embryos lacking the proprotein convertase Furin. Development 125, 4863–4876.
Ryan, A.K., Blumberg, B., Rodriguez-Esteban, C., Yonei-Tamura, S., Tamura, K., Tsukui, T., de la Pena, J., Sabbagh, W., Greenwald, J., Choe, S., Norris, D.P., Robertson, E.J., Evans, R.M., Rosenfeld, M.G., Ispisúa Belmonte, C.J., 1998. Pitx2 determines left–right asymmetry of internal organs in vertebrates. Nature 394, 545–551.
Sampath, K., Cheng, A.M., Frisch, A., Wright, C.V., 1997. Functional differences among *Xenopus* nodaL–Related genes in left–right axis determination. Development 124, 3293–3302.
Skarnes, W.C., Moss, J.E., Hurtley, S.M., Beddington, R.S., 1995. Capturing genes encoding membrane and secreted proteins important for mouse development. Proc. Natl Acad. Sci. USA 92, 6592–6596.
Snell, G.D., 1941. The early embryology of the mouse. Snell, G.D. (Ed.), Biology of the Laboratory Mouse, Blakiston, Philadelphia, PA, pp. 1–54.
St. Amand, T.R., Ra, J., Zhang, Y., Hu, Y., Baber, S.I., Qiu, M., Chen, Y., 1998. Cloning and expression pattern of chicken Pitx2: a new component in the SHH signaling pathway controlling embryonic heart looping. Biochem. Biophys. Res. Commun. 247, 100–105.
Stoykova, A., Fritsch, R., Walther, C., Gruss, P., 1996. Forebrain patterning defects in Small eye mutant mice. Development 122, 3453–3465.
Stoykova, A., Chowdhury, K., Bonaldo, P., Torres, M., Gruss, P., 1998. Gene trap expression and mutational analysis for genes involved in the development of the mammalian nervous system. Dev. Dyn. 212, 198–213.
Supp, D.M., Witte, D.P., Potter, S.S., Brueckner, M., 1997. Mutation of an axonemal dynein affects left–right asymmetry in inversus viscerum mice. Nature 389, 963–966.
Supp, D.M., Brueckner, M., Kuehn, M.R., Witte, D.P., Lowe, L.A., McGrath, J., Corrales, J., Potter, S.S., 1999. Targeted deletion of the ATP binding domain of left–right dynein confirms its role in specifying development of left–right asymmetries. Development 126, 5495–5504.
Tajbakhsh, S., Houzelstein, D., 1995. In situ hybridization and beta-galactosidase: a powerful combination for analysing transgenic mice. Trends Genet. 11, 42.
Tam, P.P., Meier, S., Jacobson, A.G., 1982. Differentiation of the metameric pattern in the embryonic axis of the mouse. II. Somitomeric organization of the presomitic mesoderm. Differentiation 21, 109–122.
Thisse, C., Thisse, B., 1999. Antivin, a novel and divergent member of the

TGFbeta superfamily, negatively regulates mesoderm induction. Development 126, 229–240.

Walther, C., Gruss, P., 1991. Pax-6, a murine paired box gene, is expressed in the developing CNS. Development 113, 1435–1449.

Wehr, R., Mansouri, A., de Maeyer, T., Gruss, P., 1997. Fkh5-deficient mice show dysgenesis in the caudal midbrain and hypothalamic mammillary body. Development 124, 4447–4456.

Wijnholds, J., Chowdhury, K., Wehr, R., Gruss, P., 1995. Segment-specific expression of the neuronatin gene during early hindbrain development. Dev. Biol. 171, 73–84.

Zhou, X., Sasaki, H., Lowe, L., Hogan, B.L., Kuehn, M.R., 1993. Nodal is a novel TGF-beta-like gene expressed in the mouse node during gastrulation. Nature 361, 543–547.